

First-principles molecular dynamics of liquid cesium and rubidium

Benedito José Costa Cabral

*Departamento de Química, Faculdade de Ciências de Lisboa, Rua Ernesto Vasconcelos, Bloco C1, 1000 Lisboa, Portugal
and Centro de Física da Matéria Condensada, Avenida Professor Gama Pinto 2, 1699 Lisboa, Portugal*

José Luís Martins

*Departamento de Física, Instituto Superior Técnico, Avenida Rovisco Pais, 1000 Lisboa, Portugal
and Instituto de Engenharia de Sistemas de Computadores, Rua Alves Redol 9, Apartado 13039, 1000 Lisboa, Portugal*

(Received 8 August 1994)

We simulate several states of liquid cesium and rubidium with first-principles molecular dynamics. The Hellmann-Feynman atomic forces are obtained from a quantum-mechanical calculation of its electronic structure based on the local density approximation of the density-functional formalism and using the pseudopotential plane-wave method. We compare our results with experimental data and other theoretical predictions for the structure and dynamics of liquid cesium and rubidium. We find a good agreement between our first-principles results, other theoretical predictions, and experiment.

I. INTRODUCTION

First-principles molecular dynamics was pioneered by Car and Parrinello in 1985 (Ref. 1) opening new ways for the simulation of systems in condensed phase. In recent years, numerous applications of this method² and some new developments have been reported.³ In general, first-principles molecular dynamics is based on the determination of atomic forces using density-functional-theory calculations of the electronic structure. The dynamics of the system is then generated by integration of the motion equations through algorithms used in classical molecular-dynamics simulations.⁴

The main characteristic and advantage of first-principles molecular dynamics is that it avoids the difficult task of constructing an adequate potential to model the interactions in condensed phases. Thus, an important number of applications of this approach has been directed to the simulation of liquids,^{3,5-8} amorphous systems,⁹⁻¹¹ and clusters^{12,13} for which the construction of an interaction potential in condensed phases is extremely difficult or even impossible. The most serious limitation of first-principles molecular dynamics is that with present computational time resources the number of particles used in the simulations is of the order of 100 and the dynamics lasts a few picoseconds. Another limitation of the original Car-Parrinello method is related to the use of a fictitious Lagrangian dynamics to describe the evolution of the electronic degrees of freedom which makes difficult the application of the method when energy transfer between electronic and ionic degrees of freedom occurs,^{14,15} as for example, in the simulations of metallic systems. In this sense, the development of first-principles molecular dynamics without fictitious electronic dynamics has been important.^{3,5,6,8} Some review articles on the development of first-principles molecular dynamics have appeared recently.^{2,16,17}

Liquid alkali metals have been studied by first-principles molecular dynamics. Hellmann-Feynman molecular dynamics of Li (Ref. 3) and Na (Refs. 18, 6) have been reported. In the present study we are reporting first-principles molecular-dynamics simulations of the heavier alkali metals cesium and rubidium. We have discussed structural and dynamical properties of Cs and Rb and compared our results with experimental information and other theoretical predictions. Cs (Refs. 19-25) and Rb (Refs. 22, 24-38) have been the subject of experimental and theoretical studies. Computer simulations using classical molecular dynamics of Cs (Refs. 19, 20, 24, 25) and Rb (Refs. 25, 31-34, 36, 37) and first-principles molecular dynamics of Rb (Ref. 38) have been reported. The importance of carrying out first-principles molecular dynamics of liquid metals is well known. It is related to the fact that pair pseudopotentials used in classical simulations are thermodynamically dependent, reflecting the correlations between ionic and electronic degrees of freedom in these systems. This limitation of the classical approach to model liquid metals emphasizes the importance of analyzing the behavior of these systems at lower densities, closer to the critical point where some differences between theoretical and experimental results have been observed. In order to discuss the performance of first-principles methods to model situations where the adequacy of the classical approach has been questioned, we have selected several thermodynamic states of liquid Cs and Rb including lower-density thermodynamic states, much above the melting point.

II. THEORETICAL FRAMEWORK AND COMPUTATIONAL DETAILS

A. Theoretical framework

In the density-functional formalism the electronic energy of the ground state of a system is written

$$U(\mathbf{R}_1, \dots, \mathbf{R}_n) = \min_{\rho} \left\{ \sum_{i < j} \frac{Z_i Z_j}{|\mathbf{R}_i - \mathbf{R}_j|} - \int \sum_i \frac{Z_i}{|\mathbf{R}_i - \mathbf{r}|} \rho(\mathbf{r}) d^3 r + F[\rho] \right\}, \quad (1)$$

where \mathbf{R}_i are the nuclear coordinates, Z_i the nuclear charge, and F is a universal functional of the electron density ρ . The minimization of this equation gives the ground state energy of the corresponding many-electron Schrödinger equation.^{39,40} However, the exact F is not known and most interest in the formalism is due to the success of the local-density approximation for this quantity,

$$F^{\text{LDA}}[\rho] = T_0[\rho] + \iint \frac{\rho(\mathbf{r})\rho(\mathbf{r}')}{|\mathbf{r} - \mathbf{r}'|} d^3 r d^3 r' + \int \rho(\mathbf{r}) \epsilon_{\text{xc}}(\rho(\mathbf{r})) d^3 r, \quad (2)$$

where $T_0[\rho]$ is the kinetic energy of the ground state of a system of noninteracting electrons with electron density $\rho(\mathbf{r})$ and $\epsilon_{\text{xc}}(\rho)$ is the exchange and correlation energy per electron of a homogeneous electron gas with density ρ .

The practical application of the density-functional formalism to molecular-dynamics simulations requires a very efficient computational method to calculate $U(\mathbf{R}_1, \dots, \mathbf{R}_n)$ and its derivatives with respect to the ionic positions. Once those are known we can use a standard algorithm to integrate the nuclear equations of motion,

$$M_i \mathbf{R}_i = -\nabla_{\mathbf{R}_i} U(\mathbf{R}_1, \dots, \mathbf{R}_n). \quad (3)$$

Currently, using first-principles molecular dynamics it is possible to simulate for a few picoseconds systems with ~ 50 atoms in a workstation and ~ 500 atoms in powerful parallel machines.

The time step of Car-Parrinello simulations (~ 0.1 fs) is dictated by the fast fictitious electronic dynamics, and is much smaller than the time step of classical molecular-dynamics simulations (~ 5 fs). The iterative methods^{2,3,5,6} which avoid the deviations from the adiabatic conditions which occur in the Car-Parrinello approach allow the generation of the ionic dynamics using the same time step as the classical molecular-dynamics simulations, compensating for the additional computational load of minimizing explicitly the electronic energy functional for each ionic configuration.³

B. Computational details

The energy was represented by the local-density Kohn-Sham energy functional [Eqs. (1)–(3)] in the plane-wave pseudopotential formalism. To represent the core-valence electrons interactions we have used a pseudopotential generated by the Trouiller-Martins method.⁴¹ The availability of smooth pseudopotentials

is important to reduce the required size of the plane-wave expansion.^{41–43} The reference configurations were the ground state calculated with semirelativistic corrections and including partial core corrections.⁴⁴ The pseudopotential has been transformed into a nonlocal form using a procedure proposed by Kleinman and Bylander⁴⁵ with s nonlocality. Table I reports the results for some solid state properties of Cs and Rb. For Cs the predicted results using a pseudopotential including s and p components with a core radii of, respectively, 4.4 and 4.98 a.u. give a good description of the solid state. For Rb we used core radii of 4.1 and 4.4 a.u. for, respectively, s and p wave functions. As is illustrated in Table I, very good agreement between theoretical and experimental results is observed for the Rb solid phase. Since we are dealing with alkali metal atoms, we tried a local pseudopotential constructed from the s wave functions. Although this speeds up the calculations, the predictions of solid state properties with this simplified local pseudopotential are not in good agreement with experiment. For the liquid-state molecular-dynamics simulations we have used the nonlocal pseudopotentials with s and p components, a plane-wave cutoff energy of 4 Ry and 5 Ry for Cs and Rb, respectively, and the single γ point of the Brillouin zone. The large Hamiltonian matrices are diagonalized with an iterative scheme.⁴⁶

The Hellmann-Feynman forces, derivatives with respect to the ionic positions of the converged ground state energy functional, have been used to generate the ionic dynamics. The equation of motions have been integrated using the Beeman algorithm⁴⁷ which allows a good energy conservation. The simulations have been carried out with 54 atoms in a supercell. This number of particles is small compared to classical molecular-dynamics simulations, limiting, for example, the range of the radial distribution functions that can be studied to ~ 9 Å, but is typical of current first-principles molecular-dynamics simulations. For cesium we have used a time step of 1000 au which corresponds to 2.42×10^{-14} s. We have carried out a molecular-dynamics simulation of 300 time

TABLE I. Structural and cohesive properties of Cs and Rb calculated for the bcc solid: lattice constant a_0 , bulk modulus B_0 , and cohesive energy per atom E_c . We show that a local pseudopotential does not describe correctly the solid phase.

	Cs	[Xe]6s ¹	[Xe]6s ¹ 6p ⁰	Experimental
a_0 (Å)	5.43	6.18	6.05	6.05
B_0 (GPa)	4.23	2.77	1.43	1.43
E_c (eV/atom)	1.3	0.8	0.8	0.8
	Rb	[Kr]6s ¹	[Kr]6s ¹ 6p ⁰	Experimental
a_0 (Å)	4.98	5.59	5.59	5.59
B_0 (GPa)	5.46	3.56	1.43	1.43
E_c (eV/atom)	1.37	0.84	0.85	0.85

steps, the first 100 steps corresponding to equilibration. For rubidium the time step was 500 atu and a total of 300 time steps have been performed, the first 100 steps corresponding to equilibration. We have started from a Maxwellian velocity distribution function which has been rescaled roughly every five steps during the equilibration phase. Towards the end of the equilibration phase the temperature corresponded to the desired value and the effect of rescaling was small, showing that we were close to equilibrium. After the equilibration phase we observed excellent energy conservation in our microcanonical ensemble simulation, showing that our time step is sufficiently small for an accurate integration of the ionic equations of motion. Details of the energy conservation in our algorithm have been previously discussed.³

III. RESULTS AND DISCUSSION

The study of liquid metals at different thermodynamic conditions is important to assess the adequacy of a particular approach to model these systems. It is known that in the case of liquid metals the state dependence of the interatomic forces makes difficult a conventional treatment of these systems based on simple model potentials. This problem is certainly more difficult to solve for expanded liquid metals for which the liquid-gas transition occurs almost simultaneously with the metal-nonmetal transition. Table II reports the thermodynamic states of liquid Cs and Rb simulated in this study.

A. Cesium

There is experimental evidence that along the liquid-vapor coexistence curve of Cs,^{22,23} the mean interparticle distance remains almost constant whereas an im-

portant change in the numbers of nearest neighbors is observed. Thus, from the melting point (temperature $T_m = 301$ K, density $d_m = 1.83$ g cm⁻³) to the critical point ($T_c = 1924$ K, $p_c = 92.4$ bars, $d_c = 0.38$ g cm⁻³) the positions of the first maximum and minimum of the radial distribution functions, $g(r)$, are ~ 5.5 Å while the mean coordination number Z , calculated by integration of $g(r)$ up to the first minimum, varies from ~ 15 to ~ 4 .²³ These results reflect the formation of clusters at lower densities.^{22,23} This clustering process is related to the liquid-gas and metal-nonmetal transition mechanisms.²³ Using the mean coordination numbers Z for our three states, a fit to the function $Z = \alpha d + \beta$ where d is the density leads to $\alpha = 6.26$ and $\beta = 2.2$. Thus, at the Cs critical density we predict that Z_c is 4.6. A model calculation involving a fixed array of atoms, with only the number of bonds changing,²³ predicts that Z_c is 2.7. However, this value is a lower limit since it is expected that local clustering, which is not included in the simplified lattice model but occurs at lower densities, should increase that value. We compare our results with the experimental data for $g(r)$ in Fig. 1 and in Table II we report some characteristics of the Cs structure for the different thermodynamic states. Distances of closest approach (R_c) are in the 3.7–3.4 Å range. The positions of the first maximum are almost constant and about 5.2 Å, in good agreement with experimental data. The agreement with experiment is also very good for the positions of the first minima which are at about 7.4 Å. The mean coordination numbers decrease linearly with the density which is also the experimental behavior. The only small discrepancies between first-principles and experimental results concern the height of the first maxima and the short range behavior of $g(r)$ at 973 K.

Recent studies on the dynamics of liquid Cs have been reported.^{19–22,24} From the mean square displacement, presented in Fig. 2, we have calculated the diffusion co-

TABLE II. For three thermodynamic states of liquid Cs and Rb characterized by their temperatures T and density d , we show the pressure p , the distance of closest approach R_c , maximum R_{\max} , and minimum R_{\min} of the radial distribution function $g(r)$, coordination number Z , and diffusion coefficient D .

	Cs			Rb		
	350	573	973	350	600	1200
T (K)	350	573	973	350	600	1200
d (g cm ⁻³)	1.832	1.68	1.45	1.46	1.366	1.105
p (GPa)	0.2(6)	0.0(1)	-0.0(6)	-0.1(8)	-0.0(4)	0.1(7)
R_c (Å)	3.7	3.5	3.4	3.5	3.2	1.7
R_{\max} (Å)	5.2	5.3	5.2	4.8	4.7	5.2
$g(R_{\max})$	2.4	2.15	1.7	2.5	1.9	1.3
R_{\min} (Å)	7.4	7.3	7.4	6.8	6.8	6.9
$g(R_{\min})$	0.5	0.7	0.8	0.5	0.6	0.8
Z	13.7	12.7	11.3	13.3	12.6	10.7
D (10 ⁻⁵ cm ² s ⁻¹)	2.3	5.2	12.9	2.2	6.5	15.9
	(2.35) ^a			(2.6) ^b	(14.7) ^c	
	(1.92) ^d			(3.8) ^e		

^aExperimental value at 308 K (Ref. 21).

^bClassical molecular-dynamics prediction at 332 K (Ref. 34).

^cMolecular-dynamics result at 609.6 K (Ref. 37).

^dTheoretical value at 308 K (Ref. 24).

^eMolecular-dynamics result at 315.5 K (Ref. 37).

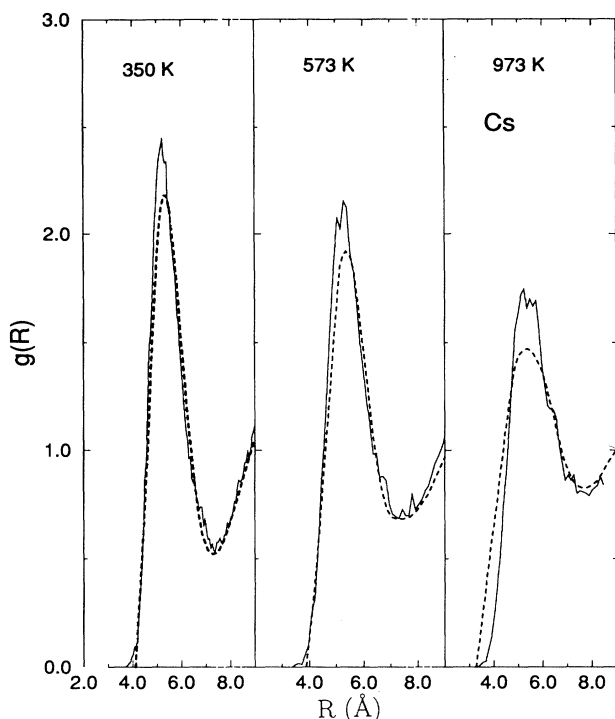


FIG. 1. Radial distribution functions $g(r)$ for liquid Cs. Solid lines are the first-principles molecular-dynamics results; dashed lines are experimental results from Ref. 22. The result at 350 K is compared with experiment at 323 K.

efficients reported in Table II. A least-squares fit to the Arrhenius form

$$D(T) = D_0 \exp(-E_a/kT)$$

leads to $D_0 = 18.71 \times 10^{-5} \text{ cm}^2 \text{ s}^{-1}$ and $E_a = 0.0631 \text{ eV}$.

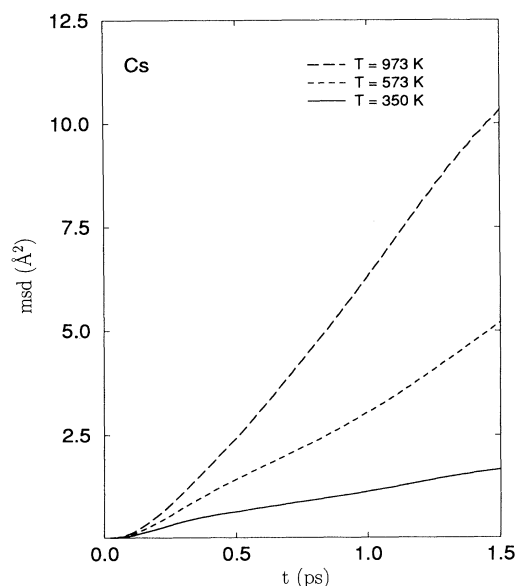


FIG. 2. The mean square displacement (msd) of liquid cesium as a function of time is shown for three different temperatures.

From the Arrhenius law the predicted value for 308 K is $1.7 \times 10^{-5} \text{ cm}^2 \text{ s}^{-1}$ which can be compared with a recent theoretical prediction from the mean square displacement ($1.974 \times 10^{-5} \text{ cm}^2 \text{ s}^{-1}$).²⁴

B. Rubidium

The structure of liquid rubidium is presented in Fig. 3 and some data on the structure are reported in Table II. The pronounced dependence of the closest approach distance on the temperature reflects the softness of the Rb core. Although the important reduction of the distance of closest approach is at 1200 K, the positions of the first maxima and minima are almost constant from 350 to 1200 K. The positions of the maxima (which are related to average interparticle distances) are in the ~ 4.8 to $\sim 5.2 \text{ \AA}$ range, in good agreement with recent experimental data.²² The behavior of the mean coordination number Z is very similar to that one observed in liquid Cs, decreasing linearly with decreasing density. Using the mean coordination number Z for our three states, a fit to the function $Z = \alpha \times d + \beta$ where d is the density leads to $\alpha = 7.3$ and $\beta = 2.66$. Thus, at the critical density of Rb (0.29 g cm^{-3}) our extrapolation predicts that Z_c is 4.7.

We observe that for structural properties of liquid Rb the agreement between theoretical studies using effective pseudopotentials and experimental Rb is dependent on the thermodynamic states. Thus, comparison between the structure factor predicted by classical molecular-

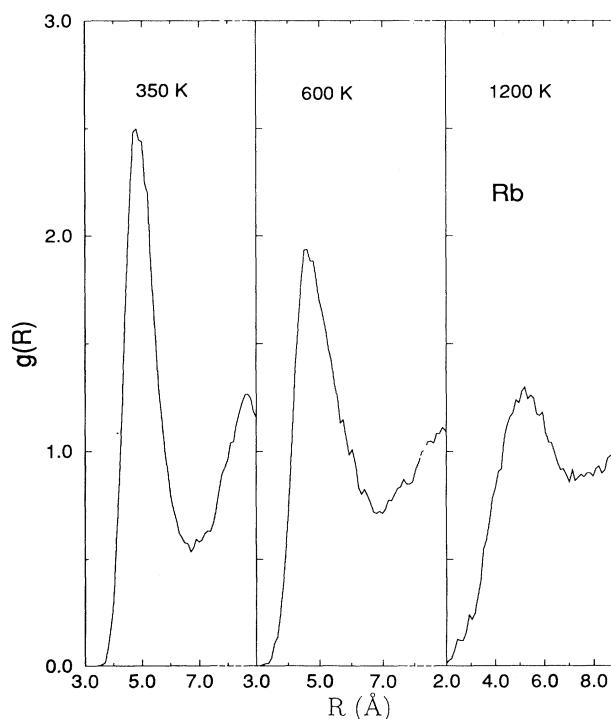


FIG. 3. The calculated radial distribution functions $g(r)$ for liquid Rb is shown for three thermodynamic states.

dynamics simulations shows that close to the melting point, computer simulation results are in good agreement with experimental data. However, for Rb at 609.6 K and for a density of 1.366 g cm^{-3} some significant differences occur.³⁷ Similarly, the static structure factors of expanded liquid Rb predicted by the optimized random phase approximation, using the Price pseudopotential and experiment, also showed some significant differences for temperatures above 1200 K, although the agreement at lower temperatures is good.³⁰

Figure 4 presents the mean square displacement for liquid rubidium. From these curves the diffusion coefficients have been calculated and are reported in Table II. Our value at 350 K ($2.2 \times 10^{-5} \text{ cm}^2 \text{ s}^{-1}$) compares well with theoretical and experimental values at temperatures close to the melting point.²⁵ The experimental value at 318 K is $2.6 \times 10^{-5} \text{ cm}^2 \text{ s}^{-1}$ and the classical molecular-dynamics prediction is $2.4 \times 10^{-5} \text{ cm}^2 \text{ s}^{-1}$.²⁵ An Arrhenius-type description of self-diffusion in liquid Rb has been questioned.³⁷ It has been suggested that the self-diffusion constants fit a T^n law with $n = 1.65$ along most of the saturated vapor pressure curve.³⁷ From our results a least-squares fit to a Arrhenius-type law gives $D_0 = 39.0 \times 10^{-5} \text{ cm}^2 \text{ s}^{-1}$ and $E_a = 0.0892 \text{ eV}$. Recently, an Arrhenius-type law has been proposed to describe the dynamics of liquid Na.⁶ There are some important differences between theoretical predictions of the diffusion coefficients for Rb which seem to be related to differences in the pair potentials used in the simulations. Thus, molecular-dynamics simulations by Tanaka³⁷ using an effective pair potential with parameters proposed by Cowley and screening parameters of Singwi predicted a diffusion coefficient much higher than that predicted by Rahman using the Price potential. The values of D from these studies are reported in Table II and they illustrate that the description of the dynamical properties of liquid Rb using classical molecular dynamics is very sensitive to the pair pseudopotentials.

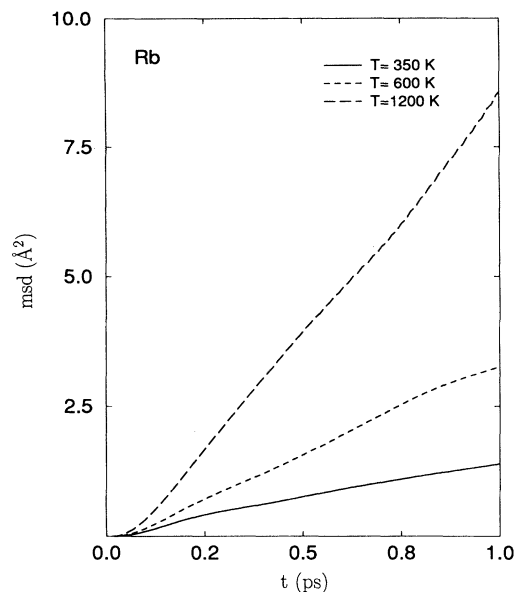


FIG. 4. The mean square displacement (msd) of liquid Rb as a function of time is shown for three temperatures

IV. CONCLUSIONS

We performed first-principles molecular-dynamics simulations of Cs and Rb for several thermodynamic states in the liquid phase. We have verified that a local pseudopotential does not predict the solid state properties correctly and all the simulations in the liquid phase have been carried with nonlocal pseudopotentials.

Our results for the structure and dynamics are in good agreement with experimental predictions. Some relevant features, such as the behavior of the mean coordination number as a function of the density, have been correctly reproduced, suggesting that the present approach is important and adequate to model expanded liquid metals.

¹ R. Car and M. Parrinello, *Phys. Rev. Lett.* **55**, 2471 (1985).
² M. C. Payne, M. P. Teter, D. C. Allan, T. Arias, and J. D. Joannopoulos, *Rev. Mod. Phys.* **64**, 1045 (1992).
³ R. M. Wentzcovitch and J. L. Martins, *Solid State Commun.* **78**, 831 (1991).
⁴ M. P. Allen and D. J. Tildesley, *Computer Simulation of Liquids* (Oxford University Press, Oxford, 1987).
⁵ T. Arias *et al.*, *Phys. Rev. B* **45**, 1538 (1992).
⁶ D. M. Bylander and L. Kleinman, *Phys. Rev. B* **45**, 9663 (1992).
⁷ G. Galli and M. Parrinello, *Phys. Rev. Lett.* **69**, 3547 (1992).
⁸ G. Kresse and J. Hafner, *J. Non-Cryst. Solids* **156-158**, 956 (1993).
⁹ D. Hohl and R. O. Jones, *Phys. Rev. B* **43**, 3856 (1991).
¹⁰ P. A. Fedders, D. A. Drabold, and S. Klemm, *Phys. Rev. B* **45**, 4048 (1992).
¹¹ M. Menon, K. R. Subbaswamy, and M. Sawtarie, *Phys. Rev. B* **48**, 8398 (1993).

¹² P. Ballone, W. Andreoni, R. Car, and M. Parrinello, *Phys. Rev. Lett.* **60**, 271 (1988).
¹³ N. Binggeli, J. L. Martins, and J. Chelikowsky, *Phys. Rev. Lett.* **68**, 2956 (1992).
¹⁴ G. Pastore, E. Smargiassi, and F. Buda, *Phys. Rev. A* **44**, 6334 (1991).
¹⁵ P. E. Blöchl and M. Parrinello, *Phys. Rev. B* **45**, 9413 (1992).
¹⁶ D. K. Remler and P. A. Madden, *Mol. Phys.* **70**, 921 (1990).
¹⁷ G. Galli, *J. Phys. Condens. Matter* **5**, B107 (1993).
¹⁸ G.-X. Qian, M. Weinert, G. W. Fernando, and J. W. Davenport, *Phys. Rev. Lett.* **64**, 1146 (1990).
¹⁹ S. Kambayashi and G. Kahl, *Phys. Rev. A* **46**, 3255 (1992).
²⁰ S. Kambayashi and G. Kahl, *Europhys. Lett.* **18**, 421 (1992).
²¹ T. Bodensteiner, Chr. Morkel, W. Gläser, and B. Dorner, *Phys. Rev. A* **45**, 5709 (1992).
²² R. Winter, C. Pilgrim, F. Hensel, C. Morkel, and W. Gläser, *J. Non-Cryst. Solids* **156**, 9 (1993).

- ²³ V. M. Nield, M. A. Lowe, and R. L. McGreevy, *J. Phys. Condens. Matter* **3**, 7519 (1991)
- ²⁴ G. Kahl, S. Kambayashi, and G. Nowotny, *J. Non-Cryst. Solids* **15**, 156 (1993).
- ²⁵ U. Balucani, A. Torcini, and R. Vallauri, *Phys. Rev. B* **47**, 3011 (1993); *J. Non-Cryst. Solids* **156**, 43 (1993).
- ²⁶ J. R. D. Copley and J. Rowe, *Phys. Rev. A* **9**, 1656 (1974).
- ²⁷ J. R. D. Copley and J. Rowe, *Phys. Rev. Lett.* **32**, 49 (1974).
- ²⁸ Y. Waseda, *Z. Naturforsch. A* **38**, 509 (1983).
- ²⁹ G. Pastore and M. P. Tosi, *Physica B* **124**, 383 (1984).
- ³⁰ G. Kahl and J. Hafner, *Phys. Rev. A* **29**, 3310 (1984).
- ³¹ A. Rahman, *Phys. Rev. A* **9**, 1667 (1974).
- ³² A. Rahman, *Phys. Rev. Lett.* **32**, 52 (1974).
- ³³ U. Balucani, R. Vallauri, T. Gaskell, and G. Mori, *Phys. Rev. A* **35**, 4263 (1987).
- ³⁴ U. Balucani, R. Vallauri, T. Gaskell, and G. Mori, *Phys. Lett.* **102A**, 109 (1984).
- ³⁵ A. Norden and D. Lodding, *Z. Naturforsch. A* **22**, 215 (1967).
- ³⁶ R. D. Mountain, *J. Phys. F* **8**, 1637 (1978).
- ³⁷ M. Tanaka, *J. Phys. F* **10**, 2581 (1980).
- ³⁸ B. J. C. Cabral and J. L. Martins, *J. Mol. Struct.* (to be published).
- ³⁹ P. Hohenberg and W. Kohn, *Phys. Rev. B* **136**, 864 (1964).
- ⁴⁰ W. Kohn and L. J. Sham, *Phys. Rev. A* **140**, 1133 (1965).
- ⁴¹ N. Trouiller and J. L. Martins, *Phys. Rev. B* **43**, 1993 (1991).
- ⁴² A. M. Rappe, K. M. Rabe, E. Kaxiras, and J. D. Joannopoulos, *Phys. Rev. B* **41**, 1227 (1990).
- ⁴³ D. Vanderbilt, *Phys. Rev. B* **41**, 7892 (1990).
- ⁴⁴ S. G. Louie, S. Froyen, and M. L. Cohen, *Phys. Rev. B* **26**, 1738 (1982).
- ⁴⁵ L. Kleinman and D. M. Bylander, *Phys. Rev. Lett.* **48**, 1425 (1982).
- ⁴⁶ J. L. Martins and M. L. Cohen, *Phys. Rev. B* **37**, 6134 (1988).
- ⁴⁷ D. Beeman, *J. Comput. Phys.* **20**, 130 (1976).